29th International Congress on Sound and Vibration
The annual congress of the International Institute of Acoustics and Vibration (IIAV)
9–13 July 2023
ICSV29

MODELLING COUPLED RIJKE TUBES BY A GREEN'S FUNCTION APPROACH

Sadaf Arabi
School of Physical and Chemical Sciences, Keele University, Staffordshire ST5 5BG, United Kingdom
email: s.arabi@keele.ac.uk

Maria Heckl
School of Physical and Chemical Sciences, Keele University, Staffordshire ST5 5BG, United Kingdom
email: m.a.heckl@keele.ac.uk

Mitigating undesired oscillations is a crucial task in dynamical systems. In this study, we investigated the occurrence of amplitude death (AD) phenomena analytically using a Green's function approach of two coupled Rijke tubes. AD depends on the effective coupling parameters, namely the time-delay and strength of the coupling that can be controlled by the length and diameter of the connecting tube, respectively. We determined the optimal settings of coupling parameters to achieve AD. If the coupling is strong enough, AD is achieved. Furthermore, the coupling position and the amplitude of the limit cycle in the uncoupled state also play a role in characterizing the AD region. For higher amplitudes, a greater strength of coupling is required at a particular time delay.

Keywords: Thermoacoustic instabilities, Green's function approach, Coupled Rijke tubes

1. Introduction

Thermoacoustic instabilities are unwanted self-sustaining oscillations caused by the feedback between heat and sound in a confined tube. It is crucial to control these high-amplitude oscillations to prevent structural damage and failures in combustion systems. Passive control mechanisms such as acoustic dampers, mufflers, baffles, and liners have been utilized to suppress high-amplitude oscillations. However, passive techniques have certain limitations due to operating conditions. Additionally, active control techniques are costly and challenging to install. Therefore, implementing a hybrid mechanism, such as coupling thermoacoustic systems, is useful.

This study investigates thermoacoustic coupling systems that lead to amplitude decrease or complete amplitude death. Although the amplitude death (AD) phenomenon due to coupled systems is rich in many fields of science, it is rare in thermoacoustic systems. Biwa et al. [1] experimentally studied coupled thermoacoustic engines to achieve amplitude death. Thomas et al. [2] used an analytical (Galerkin) approach to investigate coupled thermoacoustic systems. Based on coupling schemes and coupling parameters, they introduced particular combinations of the coupling parameters to provide amplitude death in each oscillator. A Green's function approach has been used widely to model individual thermoacoustic systems [3][4]. Here, we extend analytical investigations of thermoacoustic systems based on Green's function to coupled thermoacoustic systems.

2. Mathematical model for coupled thermoacoustic systems

In this section, we present the equations in terms of Green's function approach (Section 2.1) in the presence of the heat source (Section 2.2) and time-delay coupling (Section 2.3). We consider two individual one-dimensional Rijke tubes, coupled by a connecting tube, to model coupled thermoacoustic systems.

2.1 Modelling the resonator by Green's function approach

The tailored Green's function approach provides an integral governing equation for the acoustic field in thermoacoustic systems with source terms. It is a flexible, fast, and robust approach that provides time and frequency-domain responses. The nonlinear stability analysis of an individual thermoacoustic system has been discussed in previous studies [5]. In this study, we develop a mathematical model using the Green's function approach to model two coupled Rijke tubes.

To accomplish this, we consider two Rijke tubes, labeled (a) and (b), each with a compact flame located at x_q^a and x_q^b, respectively (see Figure 1). There are various types of coupling. However, for this study, we assume a linear time-delay coupling scheme. This coupling is created by a connecting tube between positions x_c^a in tube (a) and x_c^b in tube (b).

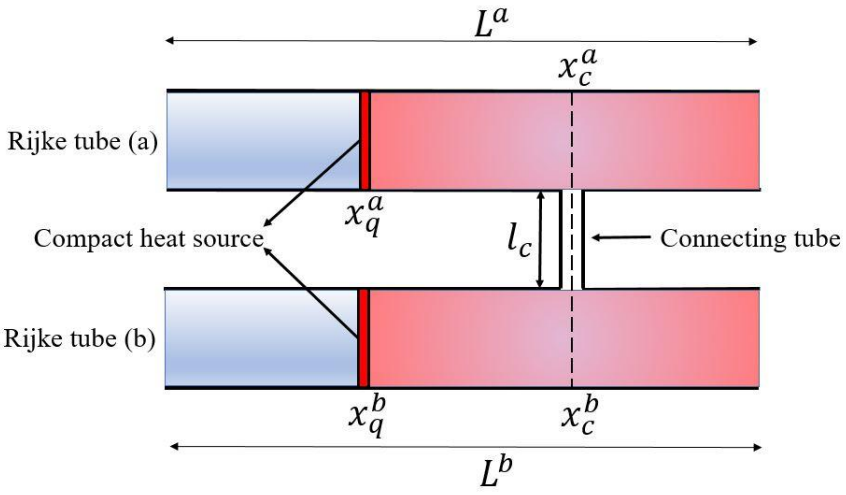

Figure 1: Illustration of the two coupled Rijke tubes (a and b) with lengths L^a and L^b. The connecting tube is attached to both tubes at x_c^a and x_c^b. The length of the connecting tube is l_c.

The tailored Green's function is the acoustic field in the resonator created by a point source at x' and time t', observed at x and time t. The governing equation is,

$$\frac{1}{c^2}\frac{\partial^2 G}{\partial t^2} - \frac{\partial^2 G}{\partial x^2} = \delta(x - x')\delta(t - t'). \tag{1}$$

For an individual Rijke tube (open ends) and temperature jump at x_q^a or x_q^b, the tailored Green's function is a superposition of modes as below,

$$G(x, x', t, t') = H(t - t')Re\sum_{n=1}^{N} g_n(x, x')e^{-i\omega_n(t-t')}. \tag{2}$$

In Eq. (2), g_n and ω_n are amplitude and frequency of mode n for each tube, respectively. The Heaviside function $H(t - t')$ in this equation shows that Green's function satisfies the causality. Due to the geometry of the resonator the frequency of mode n is determined by an eigenvalue problem, which leads to the characteristic equation $F(\omega) = 0$, where,

$$F(\omega) = e^{-ik_1 x_q} e^{-ik_2(L-x_q)} - R_L R_{21} e^{-ik_1 x_q} e^{ik_2(L-x_q)} - R_0 R_{12} e^{ik_1 x_q} e^{-ik_2(L-x_q)} - R_0 R_L e^{ik_1 x_q} e^{ik_2(L-x_q)}. \quad (3)$$

In Eq. (3), k_1 and k_2 are wave numbers in the cold and hot region of the Rijke tube with speed of sounds c_1 and c_2. The reflection coefficients of the pressure field at both ends are R_0 and R_L. Furthermore, the reflection and transmission coefficients across the temperature jump interface for the right-running waves and left-running waves are R_{12}, T_{12} and R_{21}, T_{21}, respectively.

The Green's function amplitude g_n of mode n depends on the observer and source position, and it can be calculated analytically [6]. The result is,

$$g_n(x, x') = \frac{c_2 \hat{g}(x, x', \omega)}{\omega_n F'(\omega_n)}, \quad (4)$$

where

$$\hat{g}(x, x', \omega) = \begin{cases} A(x, \omega)\, B(x', \omega) & 0 < x < x_q^{a,b} \\ B(x', \omega)\, C(x, \omega) & x_q^{a,b} < x < x'^{a,b} \\ C(x', \omega)\, B(x, \omega) & x'^{a,b} < x < L^{a,b}, \end{cases} \quad (5)$$

and

$$A(x, \omega) = T_{21}\left(R_0 e^{ik_1 x} + e^{-ik_1 x}\right), \quad (6)$$

$$B(x, \omega) = R_L e^{ik_2(L-x)} + e^{-ik_2(L-x)}, \quad (7)$$

$$C(x, \omega) = e^{ik_2(x-x_q)}\left(R_{21} e^{-ik_1 x_q} + R_0 e^{ik_1 x_q}\right) + e^{-ik_2(x-x_q)}\left(e^{-ik_1 x_q} - R_0 R_{12} e^{ik_1 x_q}\right). \quad (8)$$

The two Rijke tubes (a) and (b) may be identical or non-identical. If they are non-identical, i.e., $L^a \neq L^b$, then their frequencies differ: $\omega_n^a \neq \omega_n^b$. We will investigate the coupling effects for identical tubes.

2.2 Model for the heat release rate

In this paper, the heat source is assumed to be a compact source at $x_q^{a,b}$ and the heat release rate per unit mass is modelled by a generalised $n\tau$-model. For tube (a), this is given by,

$$q^a(x, t) = q^a(t)\delta\left(x - x_q^a\right), \quad (9)$$

where

$$q^a(t) = K\left[n_1 u_q^a(t-\tau) - n_0 u_q^a(t)\right]. \quad (10)$$

equivalent expressions hold for the heat source in tube (b).

Eq. (10) represents the nonlinear heat release rate model; it is nonlinear in that it depends on the amplitude A of the acoustic field in the tube. The amplitude-dependence occurs in the parameters n_1, n_0 (coupling coefficients) and τ (time-lag) as shown in equations (11) to (13). K represents the heat power and $\bar{u}$ is the mean velocity to normalize the acoustic field of the tube [6].

$$n_0 = \frac{1}{2}\left(g_0 - g_1 \frac{A}{\bar{u}} - 1\right), \quad (11)$$

$$n_1 = \frac{1}{2}\left(g_0 - g_1 \frac{A}{\bar{u}} + 1\right), \quad (12)$$

$$\tau = \tau_0 + \tau_2 \left(\frac{A}{\bar{u}}\right)^2. \quad (13)$$

2.3 Model for the time-delay coupling

This study focuses on the impact of time-delay coupling in identical oscillators, where coupled oscillators exhibit intriguing dynamical phenomena [7][8][9]. The connecting tube transmits sound between the two Rijke tubes with an infinite time-delay. We model each end of the connecting tube as a monopole sound source, with volume flow,

$$Q_c^a(x,t) = Q_c^a(t)\delta(x - x_c^a), \tag{14}$$

$$Q_c^a(t) = \alpha\Big(p_c^b(t-\tau_c) - p_c^a(t)\Big), \tag{15}$$

$$Q_c^b(x,t) = Q^b(t)\delta(x - x_c^b), \tag{16}$$

$$Q_c^b(t) = \alpha\Big(p_c^a(t-\tau_c) - p_c^b(t)\Big). \tag{17}$$

τ_c is the finite time it takes for the pressure field to travel inside the connecting tube and α is the strength of the time-delay coupling. These parameters can be varied in a practical situation: increasing the length of the connecting tube increases τ_c, while increasing the diameter of the connecting tube increases α.

2.4 The integral governing equation by a flame and time-delay coupling

One of the advantages of using the Green's function approach is the ability to convert a partial differential equation into an integral governing equation. This type of equation allows for a better understanding of the physical behaviour of acoustic waves in real-life scenarios, making it a more reliable and robust approach. In section (2.4.1), we demonstrate the derivation of the integral governing equation in terms of the velocity potential, considering the presence of a flame and time-delay coupling as two sources. In section (2.4.2), we utilize a numerical iteration scheme to solve the integral governing equation.

2.4.1 Derivation

Using the set up shown in Figure 1, and considering two sources within the tube, the non-homogenous acoustic analogy equation in terms of the velocity potential becomes,

$$\frac{1}{c^2}\frac{\partial^2\phi^{a,b}}{\partial t^2} - \frac{\partial^2\phi^{a,b}}{\partial x^2} = -\frac{\gamma-1}{c^2}q^{a,b}(x,t) + Q_c^{a,b}(x,t). \tag{18}$$

The heat release rate term has been determined in section (2.2), and the coupling term is shown in section (2.3). It is assumed that both forcing terms are compact at the heat source and coupling positions, respectively. The initial conditions are described at heat source position as below,

$$\phi^{a,b}(x,0) = \varphi_0^{a,b}\delta\big(x - x_q\big), \qquad \frac{\partial\phi^{a,b}(x,0)}{\partial t} = {\varphi_0'}^{a,b}\delta\big(x - x_q\big). \tag{19}$$

After many mathematical manipulations (for details, see [5]), by combining Eq. (1) and Eq. (18), the integral governing equation becomes,

$$\phi^{a,b}(x,t) = \int_{t'=0}^{t}\int_{x'=0}^{L} G^{a,b}(x,x',t,t')\, q^{a,b}(x,t)\, dx'dt' + \int_{t'=0}^{t}\int_{x'=0}^{L} G^{a,b}(x,x',t,t')\, Q_c^{a,b}(x,t)\, dx'dt' + \frac{1}{c^2}\int_{t'=0}^{t}\int_{x'=0}^{L}\left[\phi^{a,b}\,\frac{\partial^2 G^{a,b}}{\partial t'^2} - G^{a,b}\,\frac{\partial^2\phi^{a,b}}{\partial t'^2}\right]dx'\,dt'. \tag{20}$$

By evaluating the sources at the heat source position and coupling position and differentiating with respect to x, Eq. (20) leads to,

$$u^{a,b}(x,t) = \frac{\partial \phi^{a,b}}{\partial x} \tag{21}$$
$$= \int_{t'=0}^{t} \frac{\partial G^{a,b}(x,x_q,t,t')}{\partial x}\, q^{a,b}(t')dt'$$
$$+ \int_{t'=0}^{t} \frac{\partial G^{a,b}(x,x_c,t,t')}{\partial x}\, Q_c^{a,b}(t')dt'$$
$$- \frac{\varphi_0^{a,b}}{c^2}\, \frac{\partial^2 G^{a,b}\left(x,x_q,t,t'\right)}{\partial x \partial t'}\Big|_{t'=0} + \frac{\varphi_0'^{\,a,b}}{c^2}\, \frac{\partial G^{a,b}\left(x,x_q,t,t'\right)}{\partial x}\Big|_{t'=0}.$$

2.4.2 Numerical iteration method

In this section, we provide a numerical iteration method to solve Eq. (21) in a straightforward way. To this end, we expand the *x*-derivative of Green's function given in section (2.1). Hence, we define two integrals (Eq. (22) and Eq. (23)) to calculate the time evolution of mode *n*.

$$I_n^{q^{a,b}}(t) = \int_{t'=0}^{t} e^{i\omega_n^{a,b}t'}\, q^{a,b}(t')\, dt', \tag{22}$$

$$I_n^{Q^{a,b}}(t) = \int_{t'=0}^{t} e^{i\omega_n^{a,b}t'} Q^{a,b}(t')\, dt'. \tag{23}$$

By splitting the time interval into two parts and some mathematical procedures (for more details, see [5]), the resulting equations are,

$$I_n^{q^{a,b}}(t) = I_n^{q^{a,b}}(t-\Delta t) + q^{a,b}(t-\Delta t)\frac{1-e^{i\omega_n^{a,b}\Delta t}}{i\omega_n^{a,b}}\, e^{i\omega_n^{a,b}t}, \tag{24}$$

$$I_n^{Q^{a,b}}(t) = I_n^{Q^{a,b}}(t-\Delta t) + Q_c^{a,b}(t-\Delta t)\frac{1-e^{i\omega_n^{a,b}\Delta t}}{i\omega_n^{a,b}}\, e^{i\omega_n^{a,b}t}. \tag{25}$$

Substituting Eq. (22) and Eq. (23) into Eq. (21), leads to,

$$u^{a,b}(x,t) = -\frac{\gamma-1}{c^2}\, Re \sum_{n=1}^{N} G_n^{a,b} I_n^{q^{a,b}}(t) \tag{26}$$
$$+ Re \sum_{n=1}^{N} G_n^{a,b} I_n^{Q^{a,b}}(t) - Re \sum_{n=1}^{N} \frac{1}{c^2}\left(i\omega_n^{a,b}\varphi_0^{a,b} + \varphi_0'^{\,a,b}\right) G_n^{a,b}\, e^{-i\omega_n^{a,b}t},$$

where $G_n^{a,b}$ is the derivation of Green's function amplitude of mode *n* with respect to x.

3. Results and Discussions

In this section, we construct two-parameter bifurcation diagrams to analyse the influence of time-delay coupling on limit cycle amplitudes. We consider two identical Rijke tubes, although it is rare to have identical combustors in practical situations. Since this study is the primary investigation of coupled thermoacoustic systems using a Green's function approach, we begin with a simple model. In the non-identical case, the difference in lengths of the Rijke tubes leads to a difference in frequencies. The

relationship between frequency detuning and different schemes of couplings is the focus of further studies.

3.1 Effect of time-delay coupling in identical tubes

To illustrate the effects of time-delay coupling on two identical Rijke tubes, we varied the coupling parameters (τ_c, α) in coupling term presented in Section (2.3). The heat source positions are located at $x_q^{a,b} = 0.4\,m$ in both tubes, while the coupling positions are at $x_c^{a,b} = 0.7\,m$. The length of both tubes is $L^{a,b} = 2\,m$. Figure 2a shows the acoustic field in Rijke tube (a) when the coupling parameters are set to $\alpha = 0.003$ and $\tau_c = 0.012$. In this case, the coupling effect is not strong enough to quench the amplitude of the limit cycle, but a suppression in amplitude is observed. However, further increasing the strength of the coupling to $\alpha = 0.008$, as shown in Figure 3b, leads to the full mitigation of limit cycle amplitude and AD is achieved.

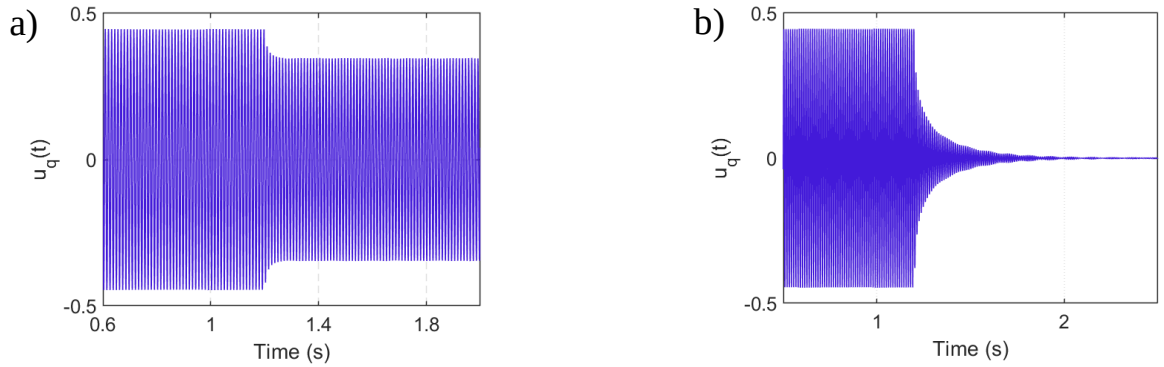

Figure 2: Time evaluation of Rijke tube (a) with coupling. a) Coupling parameters are $\alpha = 0.003$ and $\tau_c = 0.012$ and the coupling is on at t = 1.2s. b) Coupling parameters are $\alpha = 0.008$ and $\tau_c = 0.012$ and the coupling is on at t = 1.2s.

Hence, varying the coupling parameters can effectively change the oscillation state of a Rijke tube. Figure. 3, exhibits a two-parameter bifurcation diagram. It is illustrating the amplitude suppression of the limit cycle as α and τ_c are varied. The black region is related to the AD region, where a sufficient combination of the time-delay coupling can decrease the amplitude of the limit cycle to zero. Furthermore, the white region does not fully suppress the amplitude, but it is still possible to decrease the amplitude in this region.

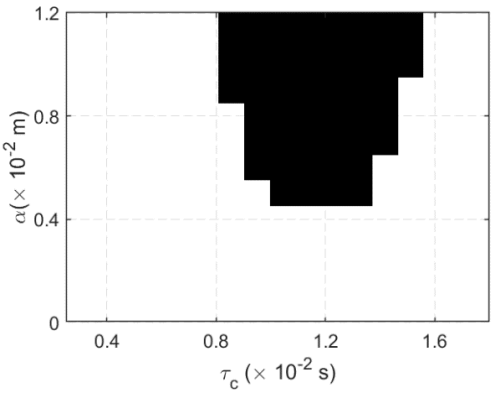

Figure 3: Two-parameter bifurcation diagram for τ_c, α and acoustic field amplitude. The black region is related to where AD is achieved. Heat source position is $x_q^{a,b} = 0.4m$ and coupling position is $x_c^{a,b} = 0.7m$. Heater power is $K^{a,b} = 3 \times 10^5 W.s.kg^{-1}$

In the next step, we moved the coupling position further away from the heat source position, setting it to $x_c^{a,b} = 1.6\,m$. Figure 4 shows the two-parameter bifurcation diagram for this case. As the coupling position moves towards the end of the tube, the heat source related to the coupling becomes more effective at quenching the amplitude of the limit cycle. In other words, achieving the AD requires smaller values for the strength of coupling. Moreover, time-delays of AD region are decreasing, which means the length of the connecting tube can be shorter. By increasing the distance between heat source position and coupling position, the coupling source acts as a sink, removing energy from the system and reducing the amplitude of the oscillations.

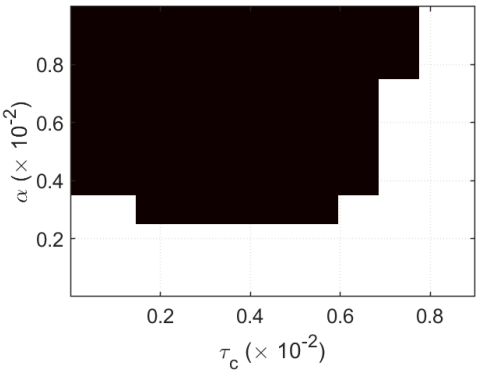

Figure 4: Two-parameter bifurcation diagram for τ_c, α and acoustic field amplitude. The black region is shown where AD is achieved. Heat source position is $x_q^{a,b} = 0.4m$ and coupling position is $x_c^{a,b} = 1.6m$. Heater power is $K^{a,b} = 3 \times 10^5 W.s.kg^{-1}$

3.2 Effect of amplitude of limit cycle on AD region

To ensure that the sets of coupling parameters are sufficient to reach AD for different amplitudes of the limit cycle, we varied the heater power. Increasing the heater power leads to an increase in the limit cycle amplitude. In this section, we increased the heater power in both Rijke tubes similarly. The heater powers of both Rijke tubes (a and b) are set to $K^{a,b} = 3 \times 10^5 W.s.kg^{-1}$ (Figure 5a). Increasing the heater power of both Rijke tubes to $K^{a,b} = 4 \times 10^5 W.s.kg^{-1}$ (Figure 5b) and $K^{a,b} = 5 \times 10^5 W.s.kg^{-1}$ (Figure 5c) shrinks the AD region. Figure 5 indicates that for higher heater power and consequently, higher limit cycle amplitude, stronger coupling is required. The plots show a moving up in AD region, that means, for a certain time-delay, it requires higher strength of coupling. In addition, the time delay range in AD region decreases as the amplitude of limit cycle increases.

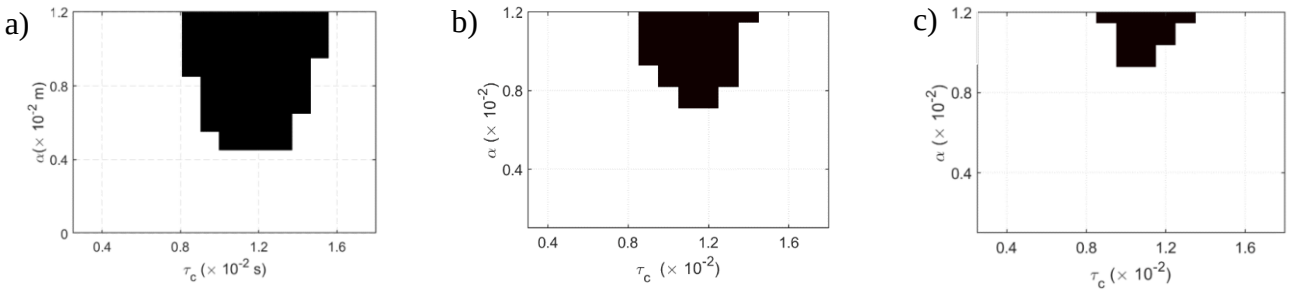

Figure 5: Two-parameter bifurcation diagrams for τ_c, α and acoustic field amplitude. a) heater power is $K^{a,b} = 3 \times 10^5 W.s.kg^{-1}$. b) heater power is $K^{a,b} = 4 \times 10^5 W.s.kg^{-1}$. c) heater power is $K^{a,b} = 5 \times 10^5 W.s.kg^{-1}$.

4. Conclusion

In this paper, we utilized a Green's function approach to simulate the behaviour of two interconnected Rijke tubes. The coupling between the tubes was achieved through a connecting tube, whose length and diameter could be adjusted based on the system's characteristics in the absence of coupling. Two coupling parameters were introduced to capture the time-delay coupling effect. By varying these parameters, we generated a bifurcation diagram that identified the ranges of coupling parameters necessary to induce an amplitude death (AD) in the system. Moreover, changing the coupling position shifted the AD region to a smaller time-delay range with weaker coupling strength. In addition to the connecting tube properties and position, the Rijke tube's limit cycle amplitude in the absence of coupling was also found to be a significant factor in selecting the coupling parameters. Specifically, in a high-amplitude limit cycle oscillation, stronger coupling was required. Lastly, we observed that the width of the time-delay coupling decreased with increasing heater power.

Acknowledgment

This work is part of the Marie Skłodowska-Curie Initial Training Network **Pol**lution **K**now-How and **A**batement (POLKA). We gratefully acknowledge the financial support from the European Commission under call H2020-MSCA-ITN-2018.

REFERENCES

[1] T. Biwa, S. Tozuka, and T. Yazaki, "Amplitude death in coupled thermoacoustic oscillators," *Phys. Rev. Appl.*, vol. 3, no. 3, p. 34006, 2015.

[2] N. Thomas, S. Mondal, S. A. Pawar, and R. I. Sujith, "Effect of time-delay and dissipative coupling on amplitude death in coupled thermoacoustic oscillators," *Chaos An Interdiscip. J. Nonlinear Sci.*, vol. 28, no. 3, p. 33119, 2018.

[3] S. Arabi and M. Heckl, "The effects of different types of noise on thermoacoustic systems using a Green's function approach," in *INTER-NOISE and NOISE-CON Congress and Conference Proceedings*, 2023, vol. 265, no. 5, pp. 2821–2830.

[4] M. A. Heckl and M. S. Howe, "Stability analysis of the Rijke tube with a Green's function approach," *J. Sound Vib.*, vol. 305, no. 4–5, pp. 672–688, 2007.

[5] A. Bigongiari and M. A. Heckl, "A Green's function approach to the rapid prediction of thermoacoustic instabilities in combustors," *J. Fluid Mech.*, vol. 798, pp. 970–996, 2016.

[6] M. A. Heckl, "Analytical model of nonlinear thermo-acoustic effects in a matrix burner," *J. Sound Vib.*, vol. 332, no. 17, pp. 4021–4036, 2013.

[7] K. Manoj, S. A. Pawar, J. Kurths, and R. I. Sujith, "Rijke tube: A nonlinear oscillator," *Chaos An Interdiscip. J. Nonlinear Sci.*, vol. 32, no. 7, p. 72101, 2022.

[8] S. Dange, K. Manoj, S. Banerjee, S. A. Pawar, S. Mondal, and R. I. Sujith, "Oscillation quenching and phase-flip bifurcation in coupled thermoacoustic systems," *Chaos An Interdiscip. J. Nonlinear Sci.*, vol. 29, no. 9, p. 93135, 2019.

[9] H. Hyodo and T. Biwa, "Stabilization of thermoacoustic oscillators by delay coupling," *Phys. Rev. E*, vol. 98, no. 5, p. 52223, 2018.